This is a repository copy of *Non-destructive detection of machining-induced white layers in ferromagnetic alloys*.

White Rose Research Online URL for this paper:
http://eprints.whiterose.ac.uk/162694/

Version: Published Version

Proceedings Paper:
Brown, M. orcid.org/0000-0002-0937-9139, Ghadbeigi, H. orcid.org/0000-0001-6507-2353, Crawforth, P. et al. (4 more authors) (2020) Non-destructive detection of machining-induced white layers in ferromagnetic alloys. In: Arrazola, P.J. and Madariaga, A., (eds.) Procedia CIRP. 5th CIRP Conference on Surface Integrity (CSI 2020), 01-05 Jun 2020, Mondragon, Spain. Elsevier , pp. 420-425.

https://doi.org/10.1016/j.procir.2020.02.065

Reuse
This article is distributed under the terms of the Creative Commons Attribution-NonCommercial-NoDerivs (CC BY-NC-ND) licence. This licence only allows you to download this work and share it with others as long as you credit the authors, but you can’t change the article in any way or use it commercially. More information and the full terms of the licence here: https://creativecommons.org/licenses/

Takedown
If you consider content in White Rose Research Online to be in breach of UK law, please notify us by emailing eprints@whiterose.ac.uk including the URL of the record and the reason for the withdrawal request.

eprints@whiterose.ac.uk
https://eprints.whiterose.ac.uk/

Available online at www.sciencedirect.com

ScienceDirect

Procedia CIRP 87 (2020) 420–425

www.elsevier.com/locate/procedia

5th CIRP CSI 2020

Non-destructive detection of machining-induced white layers in ferromagnetic alloys

M.Brown*[a,b], H.Ghadbeigi[b], P. Crawforth[c] ,R.M'Saoubi[d], A.Mantle[e], J.McGourlay[f], D.Wright[g]

[a] Industrial Doctoral Centre in Machining Science, Advanced Manufacturing Research Centre with Boeing, University of Sheffield, Rotherham, S60 5TZ, UK

[b] The University of Sheffield, Department of Mechanical Engineering, Sir Frederick Mappin Building, Mappin Street, S1 3JD, Sheffield, UK

[c] Advanced Manufacturing Research Centre with Boeing, University of Sheffield, Rotherham, S60 5TZ, UK

[d] Materials & Technology development, Seco Tools AB, SE73782 Fagersta, Sweden

[e] Manufacturing Technology, Rolls-Royce PLC, Derby, UK

[f] Rolls-Royce PLC, UK

[g] Non-destructive evaluation, Rolls-Royce PLC, Derby, UK

* Corresponding author. *E-mail address:* mobrown1@sheffield.ac.uk

Abstract

Machining-induced white layers are an undesirable surface integrity feature which, due to their physical properties, can have a direct effect on the in-service performance of aero-engine components. Typically, destructive methods such as cross-sectional microscopy are used during inspection to identify white layers. This is costly, both in terms of parts sacrificed and time-consumed. A non-destructive evaluation method could speed-up inspection and allow all parts to be inspected before entering service as well as throughout the component life cycle. The present work covers the quantitative characterization of machining-induced white layers in super chrome molybdenum vanadium steel through destructive methods in addition to Barkhausen noise non-destructive testing of the same surfaces. White layers formed by machining with severely worn inserts were measured to be up to 50% harder than the bulk material, possess nano-scale grains and can have an associated compressive residual stress state of up to -1800 MPa. Barkhausen noise testing was used to show that surfaces with a white layer formed by SPD could be detected by measuring shifts in the peak frequency of the Barkhausen noise signal, caused by the compressive near-surface residual stress state associated with the formation of white layers of this type.

© 2020 The Authors. Published by Elsevier B.V.
This is an open access article under the CC BY-NC-ND license (http://creativecommons.org/licenses/by-nc-nd/4.0/)
Peer-review under responsibility of the scientific committee of the 5th CIRP CSI 2020

Keywords: Non-destructive testing; White layer; Machining

1. Introduction

White layers are a thin, near-surface region of highly refined microstructure [1], which typically possess increased hardness relative to the bulk material [2] and large compressive [3] or tensile [4] residual stresses. This anomalous surface feature is encountered when machining difficult-to-machine aeroengine alloys, particularly when using high cutting speeds [5] or worn tools [6]. White layers have been associated with a reduction in fatigue life [7] when large tensile residual stresses are present. However, the brittle nature of the white layer [8] means that the presence of this feature on an aeroengine component would result in an immediate inspection fail regardless of residual stress state. White layers typically can form by one of two mechanisms in machined surfaces, phase transformation or severe plastic deformation (SPD) plus dynamic recrystallization [9].

The inspection of white layers is currently a destructive process wherein components are sectioned and the cross-section is imaged using optical microscopy [10]. Any level of white layer is considered an inspection failure. Microscopy, as

2212-8271 © 2020 The Authors. Published by Elsevier B.V.
This is an open access article under the CC BY-NC-ND license (http://creativecommons.org/licenses/by-nc-nd/4.0/)
Peer-review under responsibility of the scientific committee of the 5th CIRP CSI 2020
10.1016/j.procir.2020.02.065

a method for identifying white layers, is inherently costly, in terms of parts sacrificed, and time-consuming, due to the numerous process steps involved in preparing metallographic samples. At present, there is no widely researched and truly non-destructive testing (NDT) method for reliably detecting the presence of a white layer in different alloys. Therefore, there is a high demand for detecting white layers formed during machining using NDT techniques.

Early attempts at non-destructive white layer detection investigated acoustic emission testing [11] and optical scattering [12]. However, the acoustic emission study did not include the separation of effects due to the presence of white layers from effects such as surface roughness and there was no clear physical phenomena attributed to the results in the optical scattering study. There have been a number of more recent studies into the detection of machining induced white layers using Barkhausen noise (BN) methods [13, 14] in ferromagnetic materials. In BN testing, an alternating magnetic field is applied to the ferromagnetic test piece and as the magnetic field varies, the magnetic moments within the sample attempt to align with the field. However, due to domain wall movement restrictions, such as dislocations present in deformed material, the magnetization of the sample occurs in a step-wise manner. This magnetization "noise" is measured by a pick-up coil through spikes in induced current or voltage [15]. The energy required to overcome domain wall pinning and consequently the BN generated, is reported to be linked to the residual stress state [16], case-hardening [17] and grain size [18]. BN is subject to the skin depth limitations as eddy current testing, with the strength of the electromagnetic field decreasing exponentially with depth [19].

Stupakov et al. [14] were able to rank machined steel samples by the level of milling tool wear and thus white layer thickness using in-house BN equipment. It was identified that the presence of a second peak in the BN envelope (a plot of BN against magnetic field strength) could be associated with the presence of a white layer due to the increased hardness, retained austenite concentration and the favourable orientation of the martensitic matrix of the white layer. The white layers appear to have formed by the phase transformation, as evidenced in the published micrographs by the over-tempered, dark layer, beneath the white layer [14]. Dark layers are commonly associated with white layers formed by this mechanism [20]. It is, therefore, appropriate to investigate the potential for detecting white layers formed by the SPD mechanism using BN. SPD white layers typically possess a strong compressive surface residual stress state [21] and so may behave very differently under BN inspection. Additionally, commercially available BN equipment should be used to investigate whether white layer detection can be achieved without specifically designed, in-house equipment.

In this paper, the generation and characterization of super chrome molybdenum vanadium (SCMV) steel surfaces possessing a white layer is described, in terms of their microstructure, nanohardness, phase composition and residual stress, in order to outline the key properties of this surface integrity feature. The results from non-destructive Barkhausen noise inspection of the same surfaces are discussed with reference to the destructive characterization work in an attempt to identify a non-destructive method for identifying surfaces with a white layer.

2. Experimental set-up

A set of test pieces were generated through turning of SCMV steel to allow a comparison between standard destructive analysis methods and non-destructive BN inspection. The cutting parameters and tool geometry used in the cutting trials were selected to ensure samples with and without a white layer were produced. SCMV is a tempered martensitic steel used as shaft material in aeroengines and was provided for these trials by Rolls-Royce PLC. The turning operation was carried out on Cincinnati Hawk 300 lathe using a PDJNL2020K15JETL tool holder in combination with DNMG 150608 coated carbide inserts, both provided by Seco tools AB. A number of the inserts were pre-ground and re-honed by Seco tools AB to introduce artificial wear at levels of 0.15 mm, 0.25 mm and 0.5 mm on the flank face, as shown in Fig. 1 (a) and (b). Different levels of artificial wear on the inserts facilitated the generation of white layers with varying thickness, since increased wear levels have been associated with thicker white layers [6]. Cutting speeds between 60-180 m/min were used for the trials with tool wear levels varying between 0-0.5 mm. The depth of cut and feed were held constant at 0.5 mm and 0.15 mm/rev respectively, across all trials.

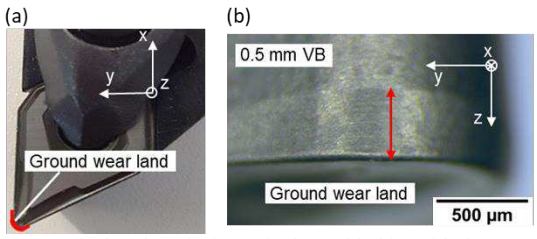

Fig. 1 – Macrographs of (a) the insert in the tool holder with the ground wear region highlighted and (b) an insert with a 0.5 mm ground wear land.

Following machining, surface roughness was quantified using a Mitutoyo Surftest SJ-210 portable surface roughness profilometer using a sampling length of 0.8 mm and an evaluation length of 4 mm over five averaged measurements in the feed direction. Workpieces were then prepared for cross-sectional optical microscopy using standard metallographic procedures. An Olympus BX51 microscope was used to capture optical micrographs of etched surfaces at 500x magnification [22] from which white layer thickness could be measured. To attempt to resolve the fine grain structure in the white layer, several samples were imaged using a high-

resolution Inspect F50 FEG-SEM. Based on the optical microscopy surface integrity inspection, a subset of surfaces encompassing the range of cutting conditions imposed, were taken forward for further analysis. X-ray diffraction (XRD) patterns were captured for these surfaces using a PANalytical Xpert[3] diffractometer with copper Kα radiation to check for phase transformation in the white layer. Nanoindentation with a triboscope nanoindenter was used to obtain cross-sectional hardness profiles through the white layer region into the bulk material, using the Oliver & Pharr [23] method, to allow the effect of hardness on Barkhausen noise inspection to be investigated. Indentations, using a 5 mN load were, applied over an 11 x 5 array (depth x width) with a size of 50 µm x 25 µm. Hardness values were normalized using the bulk hardness measured from indentations greater than 100 µm from the machined surface. Residual stress profiles were measured for cutting and feed directions using the XRD $\sin^2(\psi)$ method in combination with electropolishing, to achieve measurements at successive depths, which could be compared to BN measurement on those surfaces.

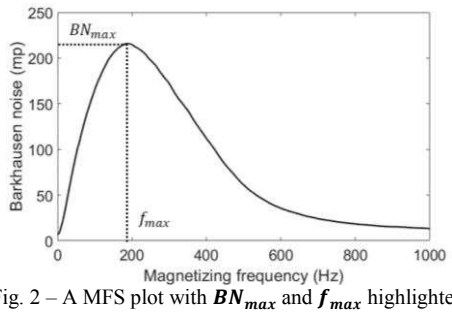

Fig. 2 – A MFS plot with $\boldsymbol{BN_{max}}$ and $\boldsymbol{f_{max}}$ highlighted.

Non-destructive BN measurements on the same turned surfaces were carried out to assess the potential for using this non-destructive method for white layer detection. In addition, different Barkhausen noise signal features were measured to establish the best measure for detecting white layers. A Stresstech Rollscan 350 Barkhausen noise analyser with a Stresstech S1-15-32-02 sensor, designed for outside diameter measurements, was used during the experiments. A high filter frequency of 200-450 kHz was used to restrict the information depth (the depth up to which most Barkhausen noise signals are detected) to 75-50 µm beneath the surface. The inspection depth was calculated using confidential material property data and the skin depth relationship described in [19]. Basic Barkhausen noise measurements at 180 Hz magnetizing frequency and 16 V_{pp}, were undertaken initially using the magnetoelastic parameter (mp) measurement mode, equivalent to the RMS of the BN signal. Following this, more advanced magnetizing frequency sweeps (MFS) were carried out. Here the frequency of the applied alternating magnetic field was increased from 0-1000 Hz at a constant voltage (16 V_{pp}) and the BN was sampled throughout. By exporting the MFS from the Viewscan software, packaged with the Rollscan equipment, to facilitate additional post-processing, two additional parameters could be extracted. BN_{max} is the maximum BN generated and f_{max} is the frequency at which this maximum BN was recorded. A typical frequency sweep is plotted in Fig. 2 with the additional parameters highlighted.

3. Results

3.1 Microstructural morphology of the white layer

Optical micrographs revealed that machined surfaces had been generated with white layers up to 11 µm thickness on the surface. Surfaces machined at low cutting speeds (60 m/min) with unworn inserts, had no observable white layer on the surface. Optical micrographs of a surface with and without a white layer are shown in Fig. 3 (a) and (b) respectively. None of the surfaces with a white layer showed evidence of a dark layer immediately beneath, as discussed in [20].

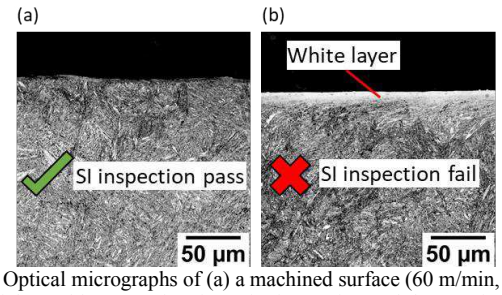

Fig. 3 – Optical micrographs of (a) a machined surface (60 m/min, 0 mm VB) which would pass surface integrity inspection and (b) a surface with a white layer (60 m/min, 0.5 mm VB) which would fail inspection.

A highly refined microstructure within the white layer was observed through high-resolution SEM imaging. Fig. 4 (a) shows that the white layer contains equiaxed grains, smaller than 200 nm on average, which contrasts the bulk microstructure visible in Fig. 4 (b) and (d).

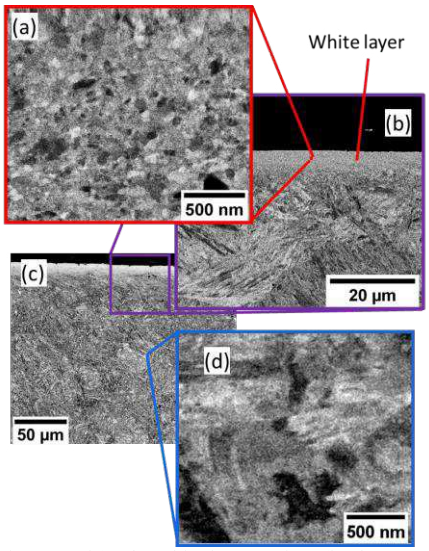

Fig. 4 – SEM images of (a) the white layer region, (b) the near-surface region and (d) the bulk microstructure. The optical image (c) is used to illustrate the relative locations of the SEM images.

3.2 XRD phase composition

A higher concentration of retained austenite is expected if the white layer had formed via the phase transformation mechanism and this would be seen as diffraction peaks associated with any austenite crystallographic planes. However, the lack of such peaks (e.g. γ(200) ~ 50°, γ(220) ~ 74°) in the XRD patterns shown in Fig. 5, indicates that the white layer formation mechanisms involved no significant phase transformation.

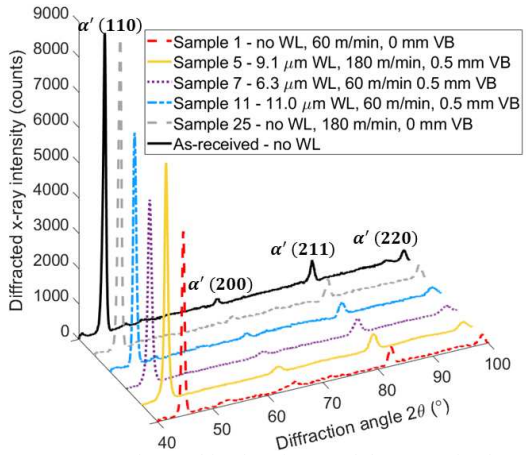

Fig. 5 – XRD patterns for machined surfaces and the as-received material with the diffraction peaks labelled with the associated crystallographic plane. The white layer (WL) thickness, cutting speeds and tool wear levels are given.

3.3 Nanoindentation

The white layer was measured to 20-45% harder than the bulk material as shown in Fig. 6, with the hardness decreasing through the white layer region from a maximum near the surface. For machined surfaces with no white layer, the hardness did not vary significantly with depth.

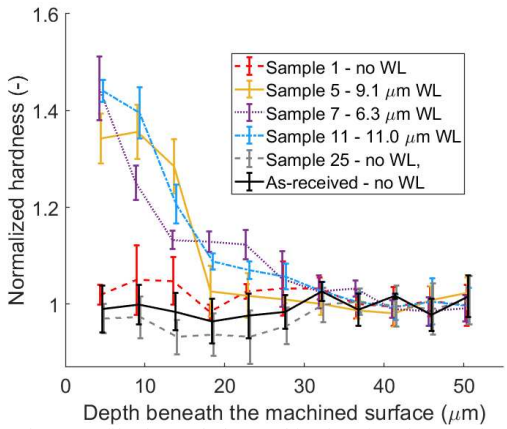

Fig. 6 – Hardness profiles beneath the machined surface for samples with and without white layers. The error bars represent one standard deviation of the hardness measurement at each depth. The hardness was normalized using the bulk material hardness.

3.4 Residual stress profiling

Residual stress profiles for a several samples, in both the feed and cutting directions, are shown in Fig. 7. It can be seen that the samples with white layers possessed significant compressive residual stresses to large depths beneath the surface. Compressive residual stresses were the largest in the feed direction. By contrast, there were tensile surface residual stresses for samples with no white layers, with small compressive residual stresses immediately beneath which decayed rapidly with depth.

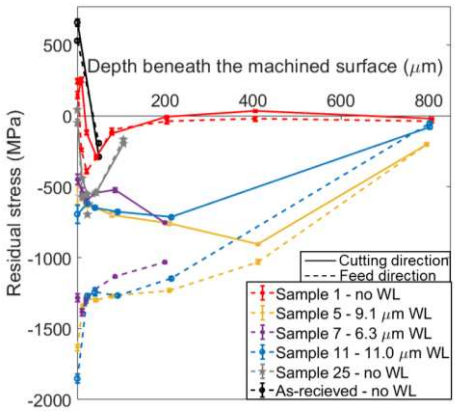

Fig. 7 – Residual stress profiles for surfaces with and without a white layer for the cutting (solid lines) and feed (dashed lines) directions.

3.5 Barkhausen noise measurements

Results from the basic BN and MFS measurements are shown in Fig. 8 (a) and (b) respectively. The BN_{max} measurements closely matched the basic BN measurements so they are not plotted here. It can be seen from Fig. 8 (a) that there is no clear relationship between the Barkhausen noise, obtained from the basic measurement capability of the Rollscan 350 unit, and the white layer thickness. By contrast, it can be seen from Fig. 8 (b) that f_{max} is different for a surface with a thick (> 2μm) white layer and there is a reduced spread in measurements.

The dependency of f_{max} upon surface roughness, hardness and residual stress is shown in Fig. 9 (a), (b) and (c) respectively. There is no apparent relationship between f_{max} and surface roughness, with a considerable range of measured f_{max} for surfaces with similar levels of surface roughness. With respect to the hardness of the surface region, f_{max} varies significantly for one of the hardened surfaces compared to the others. By contrast, the results presented in Fig. 9 (c) suggest that f_{max} increases as the residual stress becomes more tensile.

4. Discussion

It has been observed that white layers formed during turning of SCMV with worn inserts have a refined grain structure, of the order of 200 nm and smaller, this is consistent with studies in other steel alloys [2]. The lack of a visible dark

layer in optical micrographs, in addition to the absence of retained austenite peaks in the XRD patterns, can be used to infer that the white layers produced in these samples were produced by the SPD mechanism. The large compressive residual stresses add further evidence to this observation, as compressive residual stresses are associated with SPD white layers and tensile residual stresses with phase transformation white layers [21]. The compressive residual stress is not caused by white layer formation, instead both features arise from the turning process, due to the worn cutting inserts used, however, it is indicative that abnormal machining has occurred. The increased hardness of the white layers, relative to the bulk material is consistent with that measured in other steel alloys [2]. The hardened region extends beyond the white layer thickness due to strain hardening in the deformed material beneath the white layer. This deformed region, in which the microstructure is resolvable, is termed the swept grain region as the microstructure is deformed in the direction of machining.

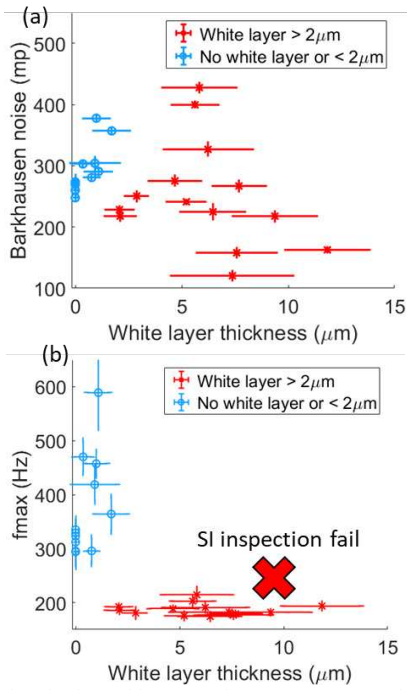

Fig. 8 – Plots of (a) basic Barkhausen noise measurement and (b) f_{max} plotted against white layer thickness.

BN NDT revealed that the basic BN measurement capability of the Rollscan 350 is not adequate for detecting the presence of a white layer. By contrast, results show that f_{max} could be used as a quick, reliable test for the presence of thick white layers in SCMV due to the clear separation between samples with white layer thicker than 2 µm and all other samples when measuring this feature of the BN signal. It should be noted that within the thick white layer region it is not possible to use the measured f_{max} to size the feature, indicating that some secondary property of the white layer is influencing the BN inspection rather than the white layers themselves.

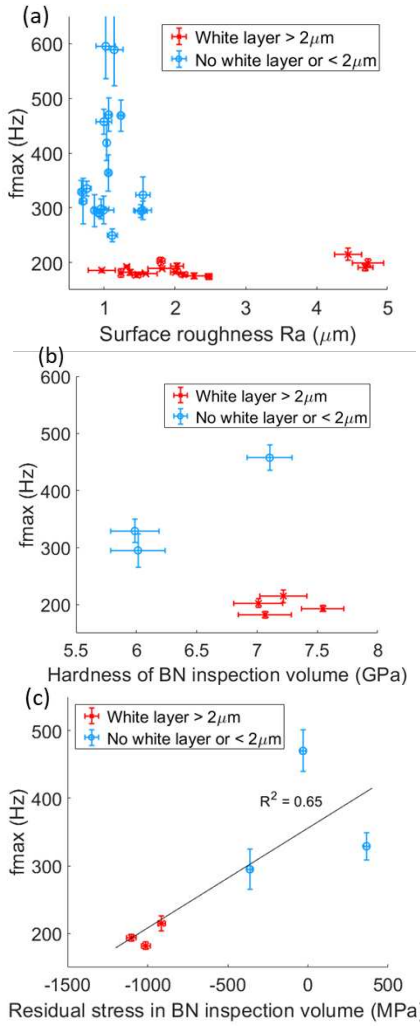

Fig. 9 – Plots of f_{max} against (a) surface roughness, (b) average hardness and (c) average residual stress in the BN inspection volume.

From the secondary properties explored in Fig. 9 (a), (b) and (c), it is the surface residual stress state which appears to have the most direct impact on measured f_{max}. Previous studies have shown that the ability of BN inspection to detect hardness changes relies on compositional change [17], thus, as the results have shown no significant compositional changes with white layer formation the impact of hardness on f_{max} is thought to be small. This is reflected by the plot in Fig. 9 (b) which shows a large change in f_{max} for two surfaces with the same hardness but different white layer states. It should be noted that the grain size will also affect BN measurements, however, the resolution limitations of SEM meant that nano-scale grain size could not be measured accurately for samples with a white layer.

Compressive residual stresses have been shown here to reduce f_{max}, i.e. decrease the frequency at which maximum BN is measured. The presence of a white layer can be therefore be inferred from the change in BN response caused by this stress state, due to the association of this surface integrity feature with large compressive stresses. For surfaces with lower compressive residual stresses, it would be expected that there would be a smaller difference in f_{max} compared to a

sample with good surface integrity. For materials with positive magnetostriction, such as most iron-carbon alloys [19], the energy required for a domain wall to overcome de-pinning, and thus generate BN, is greater under a compressive stress state [24]. The effect of this change in domain-wall pinning on f_{max} can be understood by considering that domain wall motion following a rapid increase in magnetic field strength, is not similarly rapid, there is a time-lag. This time-dependence of domain wall unpinning is described by equation (1) [25], where τ is the mean waiting time for which domain walls are pinned following a change in magnetic field strengths, f_0, is a characteristic frequency (not the magnetic field frequency), E is the activation energy for domain wall motion, k_B is the Boltzmann constant and T is the temperature.

$$\tau = \frac{1}{f_0} e^{E/k_B T} \quad (1)$$

It can be inferred, therefore, that for an increase in the domain wall energy, due to a compressive residual stress state, the time lag before domain wall motion becomes greater. At higher magnetic field frequencies, there is less time for domain walls to move before the field reverses, so the BN is reduced and consequently f_{max} decreases.

5. Conclusions

White layers formed during turning of SCMV steel have been characterized using destructive and non-destructive methods. The white layers formed in this study appear to have formed via the SPD mechanism and possess nano-scale grain structure, high hardness and compressive residual stress. Non-destructive Barkhausen noise testing was undertaken and it was identified that f_{max}, the frequency at which maximum Barkhausen was generated, could be associated with anomalous surfaces. This was achieved through detection of compressive residual stresses that are associated with white layers formed by SPD when machining with worn cutting tools. As such, f_{max}, offers an improvement over the conventional measure of the RMS of the Barkhausen noise in this application and it may be possible to use BN testing as a quick non-destructive check for SPD white layers, immediately post-machining.

Acknowledgements

This research was supported by Rolls-Royce PLC and Seco Tools AB in addition to the EPSRC [grant number EP/L016257/1]

References

[1] J. Barry, and G. Byrne, "TEM study on the surface white layer in two turned hardened steels," *Materials Science and Engineering: A,* vol. 325, no. 1–2, pp. 356-364, 2002.
[2] S. Akcan, W. S. Shah, S. P. Moylan, S. Chandrasekar, P. N. Chhabra, and H. T. Y. Yang, "Formation of white layers in steels by machining and their characteristics," *Metallurgical and Materials Transactions A,* vol. 33, no. 4, pp. 1245-1254, 2002.
[3] D. Umbrello, Z. Pu, S. Caruso, J. C. Outeiro, A. D. Jayal, O. W. Dillon, and I. S. Jawahir, "The effects of Cryogenic Cooling on Surface Integrity in Hard Machining," *Procedia Engineering,* vol. 19, pp. 371-376, 2011.
[4] J. Kwong, D. A. Axinte, and P. J. Withers, "The sensitivity of Ni-based superalloy to hole making operations: Influence of process parameters on subsurface damage and residual stress," *Journal of Materials Processing Technology,* vol. 209, no. 8, pp. 3968-3977, 2009.
[5] Y. L. Chou, and C. J. Evans, "White layers and thermal modeling of hard turned surfaces," *International Journal of Machine Tools & Manufacture,* vol. 39, pp. 1863-1881, 1999.
[6] M. Brown, P. Crawforth, R. M'Saoubi, T. Larsson, B. Wynne, A. Mantle, and H. Ghadbeigi, "Quantitative characterization of machining-induced white layers in Ti–6Al–4V," *Materials Science and Engineering: A,* vol. 764, pp. 138220, 2019/09/09/, 2019.
[7] C. Herbert, D. A. Axinte, M. Hardy, and P. Withers, "Influence of Surface Anomalies Following Hole Making Operations on the Fatigue Performance for a Nickel-Based Superalloy," *Journal of Manufacturing Science and Engineering,* vol. 136, no. 5, pp. 051016 1-9, 2014.
[8] G. Poulachon, A. Albert, M. Schluraff, and I. S. Jawahir, "An experimental investigation of work material microstructure effects on white layer formation in PCBN hard turning," *International Journal of Machine Tools and Manufacture,* vol. 45, no. 2, pp. 211-218, 2005.
[9] B. J. Griffiths, "Mechanisms of White Layer Generation With Reference to Machining and Deformation Processes," *Journal of Tribology,* vol. 109, no. 3, pp. 525-530, 1987.
[10] Rolls-Royce, "Inspection standard," 2018.
[11] Y. B. Guo, and S. C. Ammula, "Real-time acoustic emission monitoring for surface damage in hard machining," *International Journal of Machine Tools and Manufacture,* vol. 45, no. 14, pp. 1622-1627, 2005.
[12] L. Daghini, J. Holmberg, M. Falkenström, L. Nyborg, E. Tam, L. Mattsson, W. H, and P. Krajnik, *Non Destructive Testing methods: Development of innovative solutions for in-line applications*, FPI suatainable production, 2014.
[13] M. Neslušan, T. Hrabovský, M. Čilliková, and A. Mičietová, "Monitoring of Hard Milled Surfaces via Barkhausen Noise Technique," *Procedia Engineering,* vol. 132, pp. 472-479, 2015/01/01/, 2015.
[14] A. Stupakov, M. Neslušan, and O. Perevertov, "Detection of a milling-induced surface damage by the magnetic Barkhausen noise," *Journal of Magnetism and Magnetic Materials,* vol. 410, pp. 198-209, 2016/07/15/, 2016.
[15] J. Gauthier, T. W. Krause, and D. L. Atherton, "Measurement of residual stress in steel using the magnetic Barkhausen noise technique," *NDT & E International,* vol. 31, no. 1, pp. 23-31, 1998.
[16] S. Santa-aho, A. Sorsa, M. Hakanen, K. Leiviskä, M. Vippola, and T. Lepistö, "Barkhausen noise-magnetizing voltage sweep measurement in evaluation of residual stress in hardened components," *Measurement Science and Technology,* vol. 25, no. 8, pp. 085602, 2014.
[17] M. Dubois, and M. Fiset, "Evaluation of case depth on steels by Barkhausen noise measurement," *Materials Science and Technology,* vol. 11, no. 3, pp. 264-267, 1995/03/01, 1995.
[18] A. Ktena, E. Hristoforou, G. J. L. Gerhardt, F. P. Missell, F. J. G. Landgraf, D. L. Rodrigues Jr, and M. Alberteris-Campos, "Barkhausen noise as a microstructure characterization tool," *Physica B: Condensed Matter,* vol. 435, pp. 109-112, 2014.
[19] B. D. Cullity, and C. D. Graham, *Introduction to magnetic materials*: John Wiley & Sons, 2011.
[20] S. B. Hosseini, K. Ryttberg, J. Kaminski, and U. Klement, "Characterization of the Surface Integrity Induced by Hard Turning of Bainitic and Martensitic AISI 52100 Steel," *Procedia CIRP,* vol. 1, pp. 494-499, 2012.
[21] S. B. Hosseini, T. Beno, U. Klement, J. Kaminski, and K. Ryttberg, "Cutting temperatures during hard turning—Measurements and effects on white layer formation in AISI 52100," *Journal of Materials Processing Technology,* vol. 214, no. 6, pp. 1293-1300, 2014.
[22] Rolls-Royce, "Inspection standard," Unpublished results.
[23] W. C. Oliver, and G. M. Pharr, "An improved technique for determining hardness and elastic modulus using load and displacement sensing indentation experiments," *Journal of materials research,* vol. 7, no. 06, pp. 1564-1583, 1992.
[24] T. Yamasaki, S. Yamamoto, and M. Hirao, "Effect of applied stresses on magnetostriction of low carbon steel," *NDT & E International,* vol. 29, no. 5, pp. 263-268, 1996.
[25] L. Néel, "Some theoretical aspects of rock-magnetism," *Advances in physics,* vol. 4, no. 14, pp. 191-243, 1955.